

## Short-Period Variations in a Great Lakes Coastal Current by Aerial Photogrammetry

LANNY A. YESKE<sup>1</sup> AND THEODORE GREEN

*Marine Studies Center, The University of Wisconsin, Madison 53706*

(Manuscript received 29 May 1974, in revised form 26 August 1974)

### ABSTRACT

Measurements of the surface velocity structure off the Keweenaw Peninsula of Lake Superior were obtained in 1971 and 1972, using aerial photography to track surface drift cards. Variations in the current structure are described at 9-min intervals, over a 45-min period of one experiment, using streamlines and isotachs extending across the entire coastal region. Speed contour irregularities and eddies of about 100 m diameter can be traced in some of the aerial sequences. Speed fluctuations of 25% of the mean flow occur frequently. The horizontal divergence and relative vorticity structure for each sequence is also calculated; magnitudes of each are up to three times that of the local Coriolis parameter. Both inshore and offshore countercurrents are observed.

The region of anticyclonic shear is typically twice as wide as the cyclonic shear region. Cross-stream velocity gradients are about three times larger than those measured in the Gulf Stream. Rossby numbers range from 0.5 to 0.8, and inertial accelerations appear to be larger than local accelerations at least 25% of the time. Horizontal eddy viscosity coefficients range from  $\pm 10^8$  to  $\pm 10^6$  cm<sup>2</sup> s<sup>-1</sup>. Geostrophic calculations based on bathythermograph sections, airborne radiometer flights and meteorological data are also discussed.

### 1. Introduction

The physics of strong ocean currents offer many intriguing problems. For many years features such as meanders, multiple currents, volume transport variations, and kinetic energy balances have been the subject of considerable research. However, their description still remains inadequate let alone our knowledge of their importance. In part, our lack of information can be traced to the difficulties involved in obtaining statistically significant data in major ocean current systems. Most conventional measurement schemes, while yielding valuable information, are limited to some extent by the lack of simultaneity and small area coverage. Projects designed to obtain simultaneous information by standard shipboard techniques are usually prohibitively expensive. In addition, dynamic features may frequently be obscured by the numerous time and space scale complexities of the problem.

The Laurentian Great Lakes are often regarded as large-scale models of the oceans. Here complicating factors such as the variation of the Coriolis parameter with latitude and westward intensification are not likely significant (Csanady, 1967). Strong coastal currents occur seasonally and are, in some respects, similar (although not dynamically analogous) to ocean currents such as the Gulf Stream. The smaller space scale of a

few kilometers allows more accurate measurement techniques, but the smaller time scale places a premium on obtaining truly synoptic data.

Satellite sensors (multi-spectral television and thermal scanners) do not as yet have the resolution necessary for measuring lake or ocean currents. However, the use of aerial photography in conjunction with surface drogues provides a means of obtaining accurate and synoptic surface current measurements over extensive coastal regions. This is evidenced by the investigations of Keller (1963), Duxbury (1967), Sonu (1972) and Wolf and Keating (1973). These and most other aerial photographic investigations have been restricted to the nearshore coastal zone where land, used to reference drogue motion, appears in the photographs.

In offshore regions, the photographs contain no ground features for reference points and the application of aerial photography has been limited. In 1971, the University of Wisconsin Marine Studies Center began using offshore buoys, precisely positioned by shore-based theodolites, to provide these photographic reference points. This permitted an examination of the fine-scale structure of coastal currents in Lake Superior (Yeske *et al.*, 1972; Yeske, 1973). The main disadvantages of the photographic method, data reduction and interpretation, have been alleviated by the development of automatic data reduction programs and the adaptation of computerized objective analysis techniques. Photographic data collected during the 1971 and 1972

<sup>1</sup> Present affiliation: Office of the Oceanographer of the Navy, Alexandria, Va. 22332.

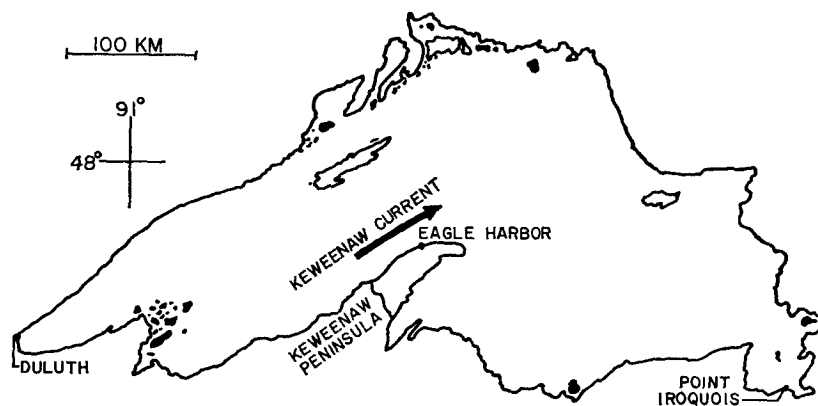


FIG. 1. Lake Superior, the Keweenaw Peninsula and the Keweenaw Current.

summer field programs have been reduced and analyzed. Among the 14 experiments conducted, several stood out as being of high quality and spanning the entire coastal current. The present paper describes some of the results obtained during a 45-min period of the 19 July 1972 experiment. For other similar data the reader is referred to Yeske (1973).

## 2. Great Lakes currents

A number of field and theoretical investigations of Great Lakes coastal currents have been performed (Csanady, 1972a, b; Mortimer, 1971; Scott *et al.*, 1969, 1971). These currents occur seasonally, and are often classified according to whether the warm water is confined to shallow, nearshore regions (the "spring"

regime), or a thermocline exists across the entire lake (the "summer-fall" regime).

Persistent currents above 1 kt occur in both regimes, and usually correlate with wind events. Changes within an inertial period are frequent and geostrophic equilibrium occurs periodically (Smith, 1972). Barotropic seiching (Platzman, 1972) and baroclinic Kelvin waves (Csanady, 1972a) appear to explain many features of these currents. Whatever the general cause, direct measurements have shown the dynamics of Great Lakes coastal currents to be both nonlinear and time-dependent.

The Keweenaw Current (Fig. 1) has been studied by the Marine Studies Center for several years (Ragotzkie, 1966; Smith and Ragotzkie, 1970). Most measurements have been made near Eagle Harbor where the flow is roughly eastward and can attain speeds over  $90 \text{ cm sec}^{-1}$  during the summer months. (Because of the latitude of Lake Superior the spring regime usually begins in July, and the summer regime in late August or early September.) Here the coastline is quite straight, and the bottom topography regular. The bottom slope is about 0.1, one of the largest in the Lakes.

In the spring regime, the sharp outer edge of the current is usually within 10 km of shore and is marked by a sharp horizontal temperature gradient [on the order of  $1^\circ\text{C} (10 \text{ m})^{-1}$ ]. In summer, these large temperature and velocity gradients are not as frequent, and the current outer edge is less well defined. Strong coastal upwelling, driven by east winds, occurs several times each summer.

Although the Keweenaw Current is re-established yearly with time and space scales much smaller than those of major oceanic currents such as the Gulf Stream, it is narrow, of relatively high velocity, lies close to shore, and may separate from the coast at the eastern end of the Peninsula. In addition, eddies, meanders and countercurrents are indicated. While any analogy between this Current and the Gulf Stream is open to criticism, it may be a means for examining the

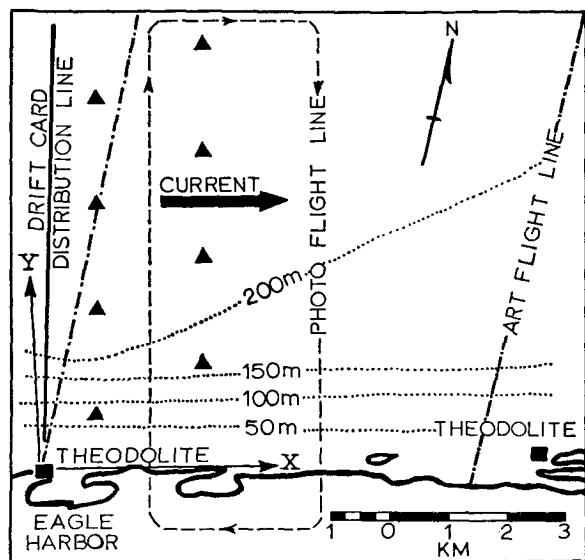


FIG. 2. The study area near Eagle Harbor, showing the location of buoys ( $\blacktriangle$ ) and theodolites ( $\blacksquare$ ) in 1972. Flight lines for photographic and radiometer operations, bottom contours and the coordinate system are also shown.

behavior of some aspects of major current systems. The kinematic comparisons between the Keweenaw Current and the Gulf Stream made below stem mainly from our desire to place the results in a broader context, and from the paucity of similar data for other bodies of water on the scale of the Great Lakes. Regardless of any broader context, the Keweenaw Current is likely one of the keys to the dynamics and general circulation of Lake Superior and is of obvious practical concern in the dispersal of pollutants introduced alongshore.

### 3. Data collection and reduction

The field procedures are illustrated in Fig. 2. The region near Eagle Harbor was selected for study because of the close proximity of the current to shore. In each experiment, drift cards (ordinary white posterboards) were distributed from small boats at intervals of 10–100 m along a line about 1 km upstream of an array of moored buoys. After the area was seeded, an aircraft equipped with a precision aerial mapping camera flew a racetrack pattern, passing over the buoy array on each outward leg and taking a series of overlapping pictures of the drift cards. Since most pictures contained no ground features, the buoys were positioned simultaneously using two shore-based precision theodolites. Up to 25 photographs were taken on one flight line, depending on the current width. The interval between aircraft passes was about 10 min with experiment

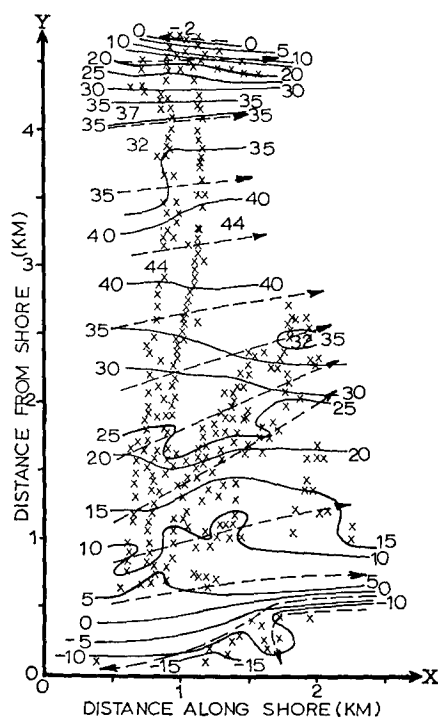


FIG. 3. Photogrammetrically derived surface speed contours (solid lines,  $\text{cm s}^{-1}$ ) and streamlines (dashed lines) off Eagle Harbor on 19 July 1972 at 0933:21.

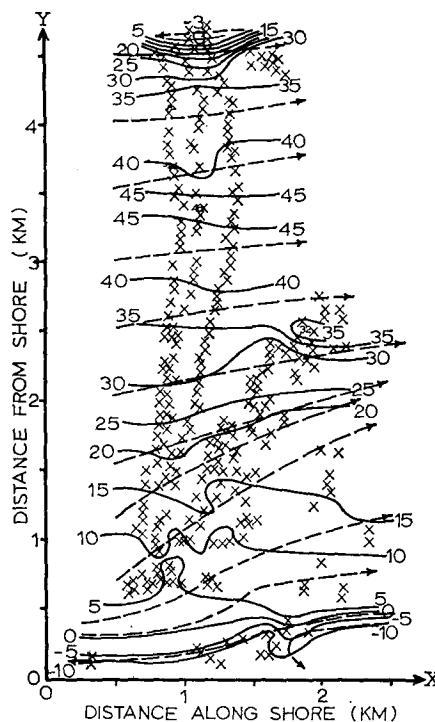


FIG. 4. As in Fig. 3 except at 0943:19.

durations ranging up to 3 h. Over 1500 drift cards were used in most experiments. Nearly all experiments were conducted under lake conditions of nearly flat calm and zero or very low wind speeds. Most of the aerial photography is supported by data from suspended current meters, bathythermographs, water level recordings, nearshore bottom-temperature recorders, and airborne radiometer flights.

Data reduction procedures (with program listings) are given in Yeske (1973). Several techniques commonly used in terrestrial photogrammetry (three-dimensional coordinate transformations and iterative polynomial strip-adjustments) are combined into a single data reduction program compatible with the measurement scheme. Corrections are applied to compensate for the short time it takes the aircraft to fly across the Current (to provide truly synoptic data), scale variations (arising from flying height oscillations and camera tilts), and inaccuracies in the measurement of photo-coordinates. Individual cards could be followed from pass to pass, and the average velocities were found by subtracting two successive drift card positions. The errors in these average velocities are less than  $2 \text{ cm s}^{-1}$  in speed and  $3^\circ$  in direction for the 10,000 velocities thus far determined. This estimate is based upon the effects of the most adverse photogrammetric conditions encountered during the project which were evaluated in the equations of a tilted photograph (Moffitt, 1967). These maximum errors are also supported by direct comparisons of the photogrammetric velocities with

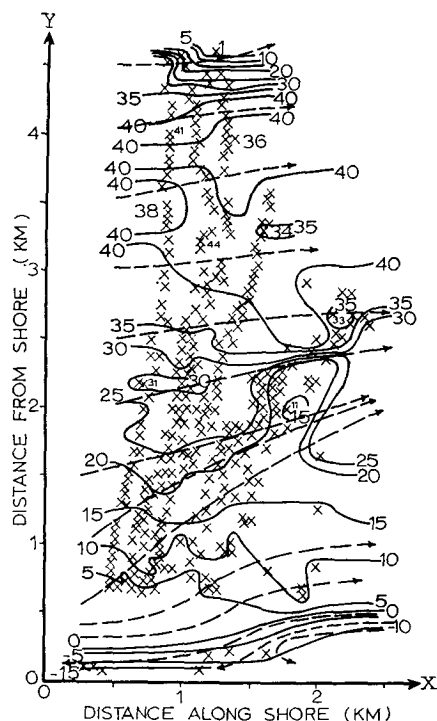


FIG. 5. As in Fig. 3 except at 0952:35.

those obtained from current meters and theodolite tracking of drogues.

#### 4. Results

##### a. Streamlines and isotachs

Five surface-velocity "snapshots" on 19 July 1972, obtained at approximately 9-min intervals, are shown in Figs. 3-7. The coordinate origin is the theodolite site at Eagle Harbor (Fig. 2). The alongshore axis ( $X$ ) is oriented along a true azimuth of  $081^\circ$  ( $081^\circ\text{T}$ ) with the transverse axis ( $Y$ ) directed cross-stream at  $351^\circ\text{T}$ . In these figures, velocity vectors were constructed at each drift card's initial position (indicated by  $\times$ ). Speeds were then contoured and streamlines drawn tangent to the velocity vectors.

The data show two westerly countercurrents (Fig. 3). The inshore countercurrent extends only 300 m offshore but attains speeds over  $15\text{ cm s}^{-1}$ . The offshore countercurrent begins at about 4.6 km and has speeds up to  $3\text{ cm s}^{-1}$ . Separating these flows is the main eastward current. Speeds increase rather gradually from 300 m to about 3.5 km offshore where a maximum of  $46\text{ cm s}^{-1}$  occurs (Fig. 4). Fig. 5 indicates significant speed changes across the current axis; three "slow" regions, with minimum speeds of 34, 36 and  $38\text{ cm s}^{-1}$  have formed. In Fig. 6 these regions appear to have merged at 3 km. On the last pass (Fig. 7) an  $11\text{ cm s}^{-1}$  speed reduction is indicated at the current axis.

Although the speed contours are quite complex, the irregularity of the  $10\text{ cm s}^{-1}$  contour 1 km offshore can be followed in all passes. Over a short time, and in the absence of wind, there is some hope that horizontal momentum can be regarded as a conservative property (see, e.g., Csanady, 1972b). We make this assumption, as momentum is the only tracer available. Then an eddy (i.e., a region of lower velocity) appears to move downstream at about  $30\text{ cm s}^{-1}$ . Another eddy at 2 km (Fig. 6) may have detached from the meander in Fig. 5. Streamlines suggest a strong convergence in this region.

##### b. The thermal bar

An important feature in the Great Lakes is the spring and fall thermal bar. In early spring the entire lake is below  $4^\circ\text{C}$ . As heating intensifies the inshore surface water warms to  $4^\circ\text{C}$ , the temperature of maximum density. This results in the sinking of surface water and the formation of a boundary, or thermal bar, between nearshore and mid-lake waters. With continued heating the bar moves away from shore and eventually merges with its counterpart on the opposite shore in late summer. The mechanism of the thermal bar and its importance to coastal circulations are not well understood (Mortimer, 1971).

Bathythermograph data obtained during the photography (Fig. 8) indicate that the thermal bar (defined by the position of the  $4^\circ\text{C}$  isotherm) separates the main eastward flow and the offshore countercurrent. The 24 h

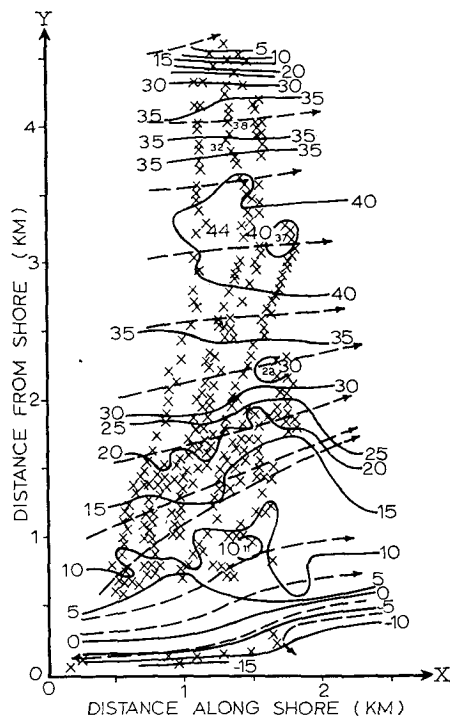


FIG. 6. As in Fig. 3 except at 1001:22.

resultant winds on 18 July were westerly at  $5 \text{ m s}^{-1}$  and probably caused the wedge-shaped thermocline below 10 m (Csanady, 1972a). On 19 July, approximately 10 h before the experiment, the winds shifted to the east and may relate to the lens-shaped thermocline above 10 m. During the photography the wind speed was about  $1 \text{ m s}^{-1}$  with 15-cm ripples on the lake. The geostrophic component of the longshore surface current was computed using standard dynamic-height calculations (Ayers, 1956), with a 60 m level of no motion. This level, a standard choice in Great Lakes work, is also the depth to which bathythermograph data were available. The surprisingly good agreement with photogrammetrically computed speeds is perhaps somewhat misleading, in view of the kinetic character of the current discussed below, and of the rather arbitrary choice of the level of no motion. However, we found similar agreement in all five photographic experiments conducted during the spring regime (Yeske, 1973).

A distinct foam line appeared in the aerial photographs 4.6 km from shore (Fig. 9) and strongly supports the presence of the thermal bar, and the downwelling tending to occur at the  $4^\circ\text{C}$  isotherm. During the experiment, the foam line moved over 100 m north. This can be seen in Fig. 9 by its position relative to Buoy R3 which moved less than 1 m cross-stream and 8 m downstream during the same period. The photogrammetrically derived positions of the line also suggest an average northerly movement rate of  $4 \text{ cm s}^{-1}$  during the first four passes of the experiment (Figs. 3-6). However, on the last pass (Fig. 7) a speed of about  $8 \text{ cm s}^{-1}$  is indicated. This apparent acceleration of the bar may have contributed to the  $11 \text{ cm s}^{-1}$  speed reduction previously discussed. In several other experiments, the current width also appeared to be inversely proportional to the current speed.

An airborne radiation thermometer flight was conducted along the entire Peninsula immediately following

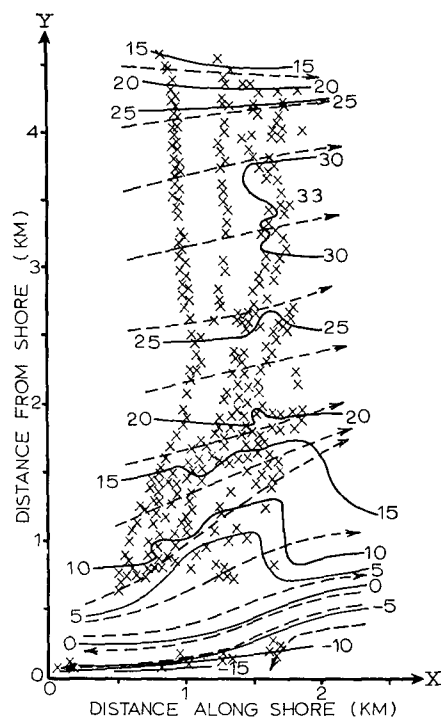


FIG. 7. As in Fig. 3 except at 1010:56.

the photography. The results (Fig. 10) show the close proximity of the current to shore (within 5 km). Large meanders are not indicated and rarely occurred during any of the 1971 and 1972 surveys.

### c. Divergence and relative vorticity

Divergence and vorticity are fundamental for examining subsurface motions and fluid circulation. Although treated in some detail theoretically, quantitative field measurements are rarely found in the oceano-

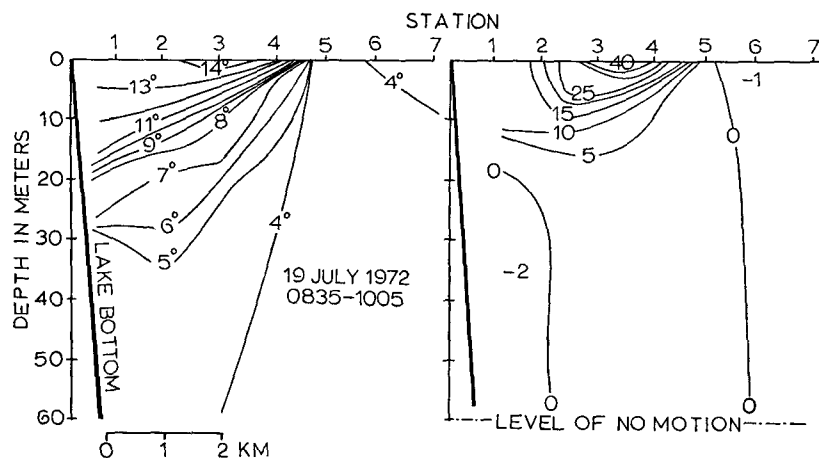


FIG. 8. Temperature cross section ( $^\circ\text{C}$ ) and longshore geostrophic currents ( $\text{cm s}^{-1}$ ) off Eagle Harbor on 19 July 1972. Positive isotachs denote flow to the east.

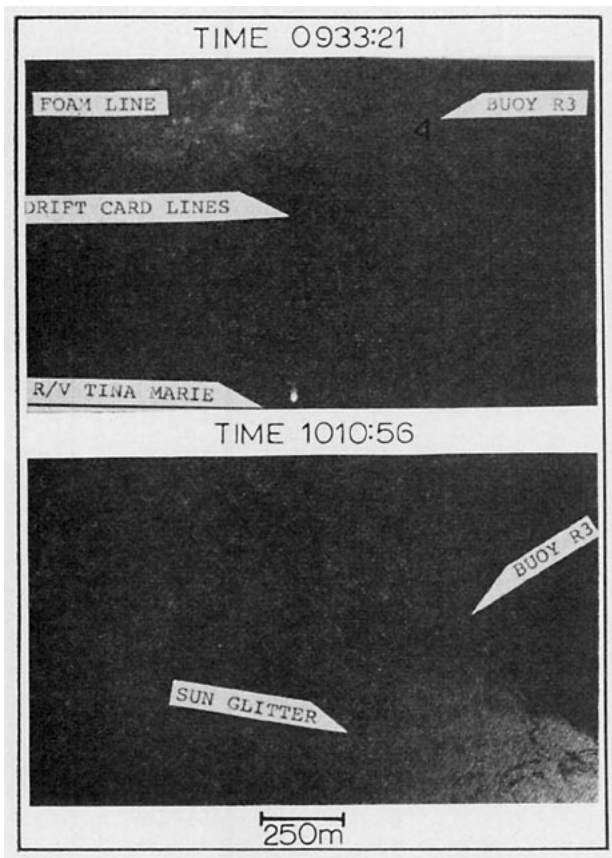


FIG. 9. Aerial photographs of the thermal bar on 19 July 1972.

graphic literature. For each "snapshot" (Figs. 3–7), the raw Lagrangian velocities were interpolated to grid points spaced 100 m apart using an objective analysis technique due to Whittaker (1974). In this method, the interpolated velocity is determined from the four raw velocities nearest the grid point, each of which is weighted by the factor  $(R-D)/(R+D)$ . Here  $R$  is the distance from the grid point to the point midway between the third and fourth closest raw velocities, and  $D$  the distance from the grid point to the raw velocity

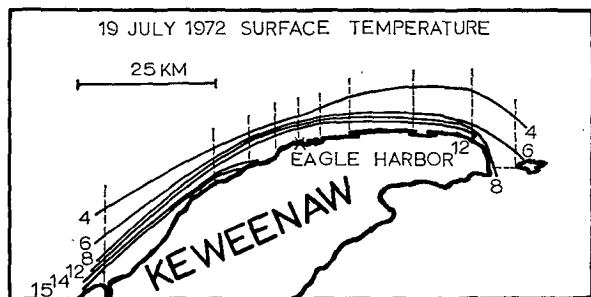


FIG. 10. Surface temperatures ( $^{\circ}\text{C}$ ) associated with the Keweenaw Current on 19 July 1972, as determined by an airborne radiation thermometer. Dashed lines denote aircraft tracks along which data were gathered.

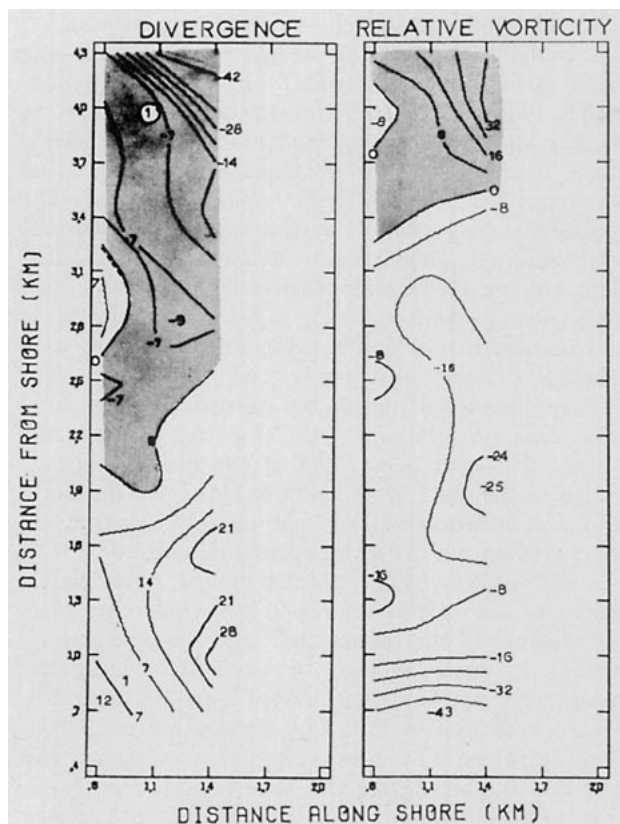


FIG. 11. Divergence and relative vorticity ( $\times 10^5 \text{ s}^{-1}$ ) off Eagle Harbor on 19 July 1972 at 0933:21.

being weighted. This method, designed for atmospheric budget studies, optimizes local features about each grid point prior to the interpolation, and preserves local features near each grid point better than more commonly used atmospheric objective analyses (e.g., Cressman, 1959). A number of tests revealed that this method minimizes data smoothing and accurately reproduces the raw data (Yeske, 1973).

The results of the horizontal divergence ( $\partial u/\partial x + \partial v/\partial y$ ) and the vertical component of relative vorticity ( $\partial v/\partial x - \partial u/\partial y$ ) calculations are given in Figs. 11–15. To facilitate pattern interpretation, convergence areas and regions of cyclonic vorticity are shaded.

Divergence generally extends from shore to about 1.5 km offshore with magnitudes up to three times that of the local Coriolis parameter. Convergence occurs from 1.5 km northward and is strongest at the thermal bar, marked by the above-mentioned foam line 4.6 km offshore. A second photographic foam line 2.4 km offshore (Figs. 14 and 15) is also present. The relative vorticity structure indicates anticyclonic shears from shore to the current axis, followed by cyclonic tendencies north.

While some of the fluctuations in the divergence and relative vorticity fields can be attributed to the

centered-difference method of computing spatial derivatives and errors in the photogrammetric method used to obtain velocities, the foam line positions agree with convergence regions. In addition, most of the changes between "snapshots" occur gradually. For example, the convergence at 4.3 km decreases rather uniformly from  $-42 \times 10^{-5}$  (Fig. 11) to  $-6 \times 10^{-5} \text{ sec}^{-1}$  (Fig. 15).

The results in Figs. 11–14 were also averaged over common areas (Fig. 16). Magnitudes are somewhat reduced from the individual patterns but still on the order of the Coriolis parameter. A measure of the statistical significance of these results can be obtained from the standard errors of the mean velocity on this day (Yeske, 1973). These  $u$  and  $v$  velocity component errors, computed at 300 m intervals across the Current and over the entire experiment, were averaged. They were then propagated into the divergence and vorticity equations using the method of Berington (1969), after which confidence intervals were calculated (Bendat and Piersol, 1971). At the 95% level, the confidence interval estimate is  $\pm 6 \times 10^{-5} \text{ s}^{-1}$ .

#### d. Speed profiles and gradients

The instantaneous downstream velocity profiles  $u(y)$  and cross-stream gradients  $\partial u / \partial y$  were calculated along a fixed line of interpolated grid points, located 1 km downstream of the Eagle Harbor theodolite and directed normal to the coastline (Fig. 17). Webster's

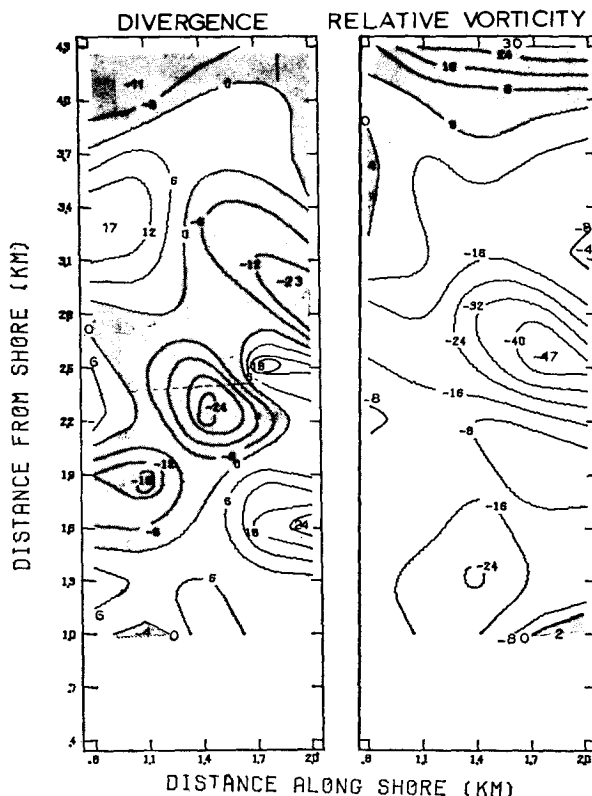


FIG. 13. As in Fig. 11 except at 0952:35.

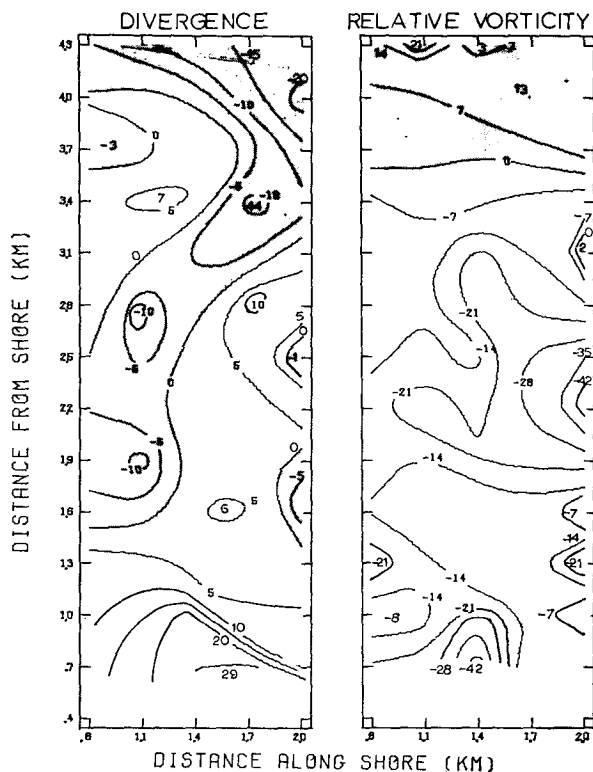


FIG. 12. As in Fig. 11 except at 0943:19.

(1961) average Gulf Stream profile in the Straits of Florida, based upon several years of observation, is asymmetric with a 28 km wide region of cyclonic shear and an average cross-stream gradient of  $3 \times 10^{-5} \text{ s}^{-1}$ . The anticyclonic region extends 59 km and has an average cross-stream gradient of  $2 \times 10^{-5} \text{ s}^{-1}$ . This extensive anticyclonic shear region has been verified in numerous sections off Miami and may result from the 50% reduction in channel width from Key West to Miami (Stommel, 1966). For the Keweenaw Current on 19 July, the average profile is also skewed with cyclonic and anticyclonic widths of about 1.5 and 3.0 km, respectively, almost exactly proportional to those of the Florida Current. Corresponding gradients are higher than Webster's observations with average values of  $11 \times 10^{-5}$  and  $9 \times 10^{-5} \text{ s}^{-1}$ . These features occur in nearly all experiments and may relate to a flow constriction imposed by the Peninsula itself.

#### e. Horizontal eddy viscosity coefficients

Horizontal eddy viscosity coefficients (Fofonoff, 1962) were computed for several experiments. These coefficients are not well known. Estimates range from  $10^3 \text{ cm}^2 \text{ s}^{-1}$  for Great Lakes currents (Csanady, 1964) to  $10^{10} \text{ cm}^2 \text{ s}^{-1}$  for the Antarctic Circumpolar Current (Fofonoff, 1962). The maximum value suggested for the Gulf Stream is about  $5 \times 10^7 \text{ cm}^2 \text{ s}^{-1}$ .

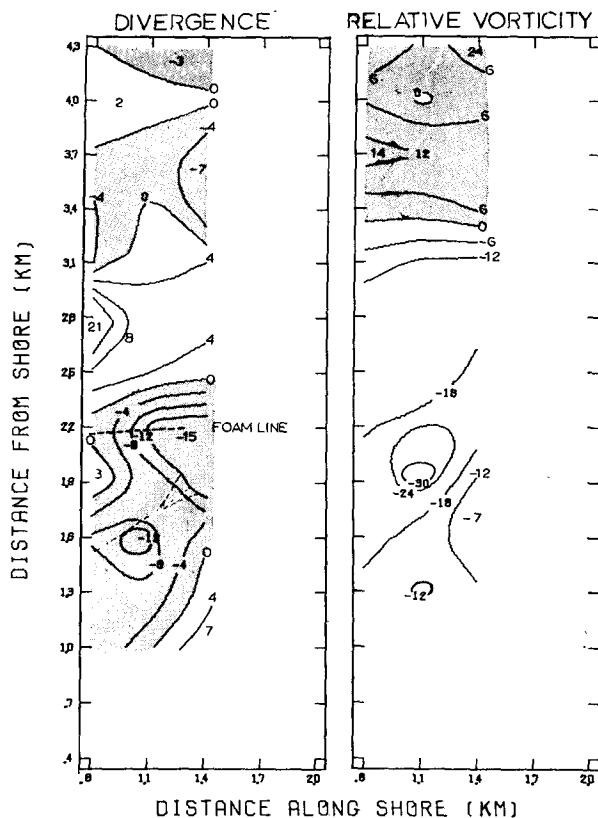


FIG. 14. As in Fig. 11 except at 1001:22.

Eddy viscosity coefficients of the form

$$K_{xx} = \frac{-\overline{u'u'}}{2\partial\bar{u}/\partial x}, \quad K_{xy} = \frac{-\overline{u'v'}}{\frac{\partial\bar{u}}{\partial y} + \frac{\partial\bar{v}}{\partial x}}, \quad K_{yy} = \frac{-\overline{v'v'}}{2\partial\bar{v}/\partial y}$$

were evaluated. To calculate these coefficients, the time-averaged momentum fluxes at interpolated grid points 300 m apart were used. The four gradients of average velocities at each grid point were obtained by taking centered differences in both the downstream and cross-stream directions. To obtain one set of coefficients for an experiment, the values at constant offshore distances were averaged in the downstream direction.

The results (Fig. 18) are typical of other days and indicate frequent changes from positive to negative values in all three coefficients. Eddy viscosities are usually between  $10^4$  to  $10^6$   $\text{cm}^2 \text{s}^{-1}$  or  $-10^4$  to  $-10^6$   $\text{cm}^2 \text{s}^{-1}$ ; the numbers of positive and negative values are nearly equal. A correlation is indicated in the  $K_{xx}$  and  $K_{yy}$  patterns from shore to about 2 km offshore. Further offshore, a correlation is suggested between  $K_{yy}$  and  $K_{xy}$ .

The calculated eddy viscosity coefficients were also averaged across the entire current, and separate averages computed for the cyclonic and anticyclonic shear zones. The results for this day and four other experiments (Table 1) indicate coefficients ranging from  $-10^3$  to  $-10^5$   $\text{cm}^2 \text{s}^{-1}$  and  $10^3$  to  $10^5$   $\text{cm}^2 \text{s}^{-1}$ . Generally,  $K_{xx}$  and  $K_{yy}$  magnitudes are on the order of  $10^5$   $\text{cm}^2 \text{s}^{-1}$ ;  $K_{xy}$  is about  $10^4$   $\text{cm}^2 \text{s}^{-1}$ . Negative  $K_{xx}$  and  $K_{yy}$  coefficients occur three times as often as positive coefficients. For  $K_{xy}$ , the number of positive and negative calculations are equal, with values usually opposite in the cyclonic and anticyclonic shear zones. Considering all experiments, the average  $K_{xx}$ ,  $K_{yy}$  and  $K_{xy}$  coefficients are about  $-10^5$ ,  $-10^4$  and  $-10^3$   $\text{cm}^2 \text{s}^{-1}$ , respectively. These are somewhat higher than other estimates for the Great Lakes and represent to our knowledge the first indication of negative eddy viscosities in the Lakes, a process not accounted for in any theoretical study. This feature is discussed in further detail in Green and Yeske (1974).

#### f. Rossby numbers and acceleration ratios

Many theoretical studies assume that the Rossby number is small, so that the inertial terms are often neglected. In regions of strong currents, Rossby numbers have not been adequately determined.

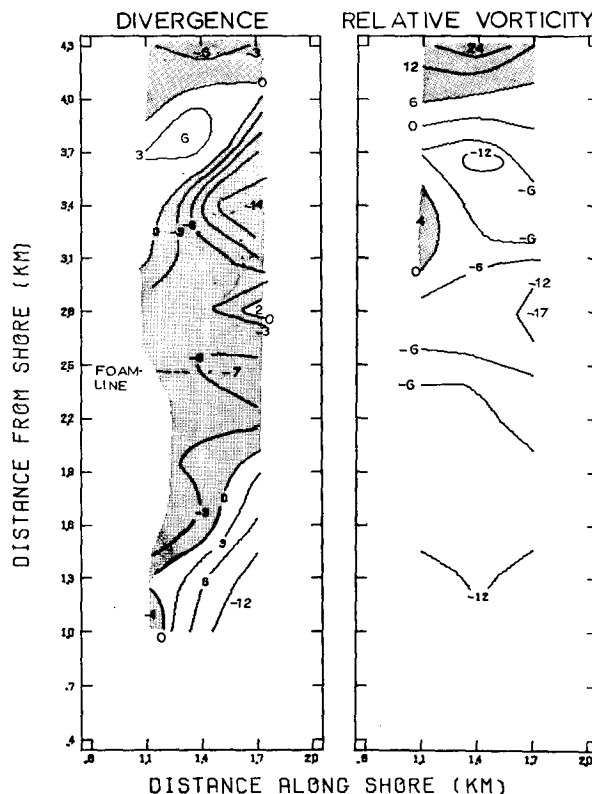


FIG. 15. As in Fig. 11 except at 1010:56.





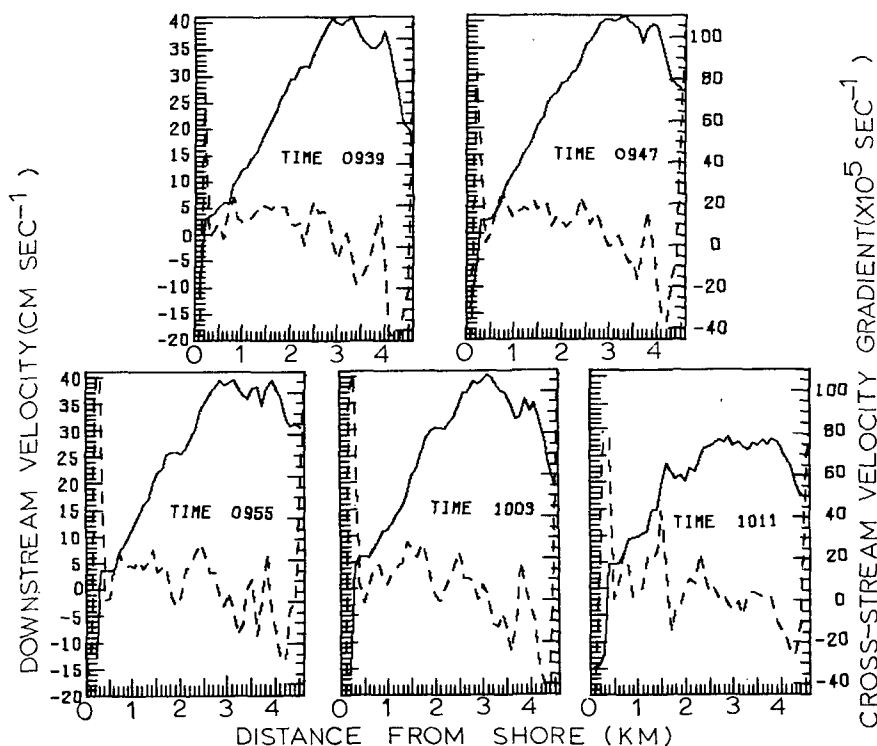


FIG. 17. Downstream velocity profiles (solid lines) and cross-stream velocity gradients (dashed lines) on 19 July 1972.

9 min. Velocity fluctuations of 25% with inshore and offshore countercurrents were observed. Horizontal divergence and relative vorticity magnitudes are often

three times larger than the local Coriolis parameter. Regions of anticyclonic shear are usually twice as wide as the cyclonic shear zone; cross-stream velocity

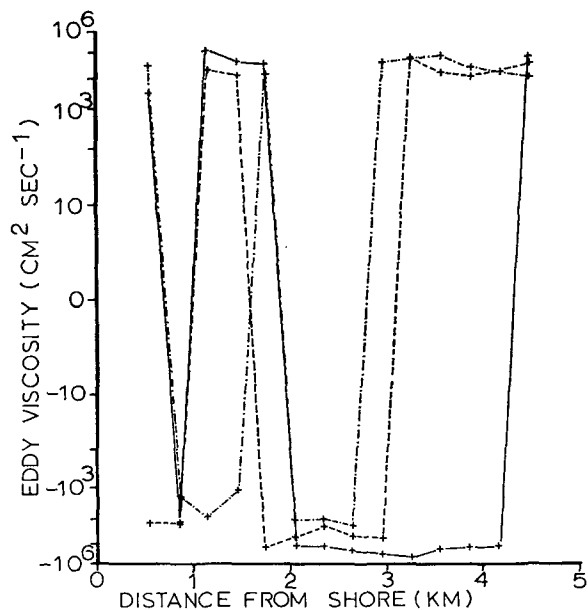


FIG. 18. Average horizontal eddy viscosity coefficients  $K_{xx}$  (solid lines),  $K_{yy}$  (dashed lines) and  $K_{xy}$  (dot-dashed lines) across the Keweenaw Current on 19 July 1972.

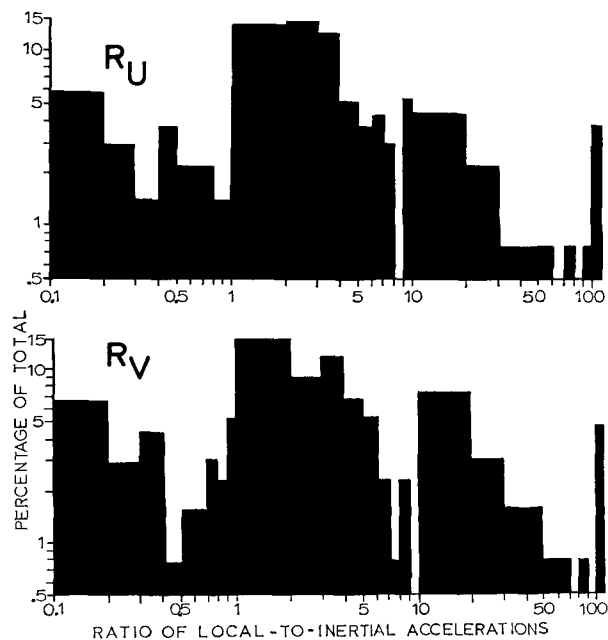


FIG. 19. Percentage of occurrence of local-to-inertial accelerations (log scale).

gradients are frequently three times larger than those observed in the Gulf Stream.

Horizontal eddy viscosity coefficients range from  $\pm 10^3$  to  $\pm 10^5$   $\text{cm}^2 \text{ s}^{-1}$  with negative coefficients dominant. The local Rossby number is about 0.6, and inertial accelerations larger than local accelerations occur at least 25% of the time.

*Acknowledgments.* This research has been supported by the National Science Foundation under Grant 33140 and to a limited extent by the National Aeronautics and Space Administration under Grant NGL 50-002-127. Programming assistance was provided by Paul Wolf, Frank Scarpance, Robert Terrell, Alan Voss and Thomas Whittaker. Bathythermograph records were analyzed by Joe Niebauer and John Gilson. Appreciation is also extended to the Marine Studies Center personnel who composed the Eagle Harbor ground crew.

## REFERENCES

- Ayers, J. C., 1956: A dynamic method for the determination of currents in deep lakes. *Limnol. Oceanogr.*, **1**, 150-161.
- Bendat, J. S., and A. G. Piersol, 1971: *Random Data: Analysis and Measurement Procedures*. Wiley-Interscience, 407 pp.
- Berington, P. R., 1969: *Data Reduction and Error Analysis for the Physical Sciences*. McGraw-Hill, 336 pp.
- Cressman, G. P., 1959: An operational objective analysis system. *Mon. Wea. Rev.*, **87**, 367-374.
- Csanady, G. T., 1964: Turbulence and diffusion in the Great Lakes. *Proc. Seventh Conf. Great Lakes Res.*, Great Lakes Res. Div., University of Michigan, 326-339.
- , 1967: Large scale motion in the Great Lakes. *J. Geophys. Res.*, **72**, 4151-4162.
- , 1972a: The coastal boundary layer in Lake Ontario: Part I. The spring regime. *J. Phys. Oceanogr.*, **2**, 3-13.
- , 1972b: The coastal boundary layer in Lake Ontario: Part II. The summer-fall regime. *J. Phys. Oceanogr.*, **2**, 168-176.
- Duxbury, A. C., 1967: Currents at the mouth of the Columbia River. *Pholog. Eng.*, **33**, 305-311.
- Fofonoff, N. P., 1962: Dynamics of ocean currents. *The Sea*, Vol. 1, Interscience, 323-396.
- Green, T., and L. A. Yeske, 1974: Horizontal turbulent energy transfer associated with a Great Lakes coastal current. Marine Studies Center Tech. Rept., University of Wisconsin (in press).
- Keller, M., 1963: Tidal current surveys by photogrammetric methods. *U. S. Coast Geod. Surv. Bull.*, **22**, 20 pp.
- Moffitt, F. H., 1967: *Photogrammetry*. Scranton, Pa., Intern. Textbook, 540 pp.
- Mortimer, C. H., 1971: Large-scale oscillatory motions and seasonal temperature changes in Lake Michigan and Lake Ontario. Center Great Lakes Research, Rept. 12, University of Wisconsin.
- Platzman, G. W., 1972: Two-dimensional free oscillations in natural basins. *J. Phys. Oceanogr.*, **2**, 117-138.
- Ragotzkie, R. A., 1966: The Keweenaw Current, a regular feature of summer circulation of Lake Superior. Dept. Meteor., Rept. 29, University of Wisconsin.
- Scott, J. T., and D. R. Landsberg, 1969: July currents near the south shore of Lake Ontario. *Proc. Twelfth Conf. Great Lakes Res.*, Intern. Assoc. Great Lakes Res., 705-722.
- , P. Jekel and M. Fenlon, 1971: Transport in the baroclinic coastal current near the south shore of Lake Ontario in early summer. *Proc. Fourteenth Conf. Great Lakes Res.*, Intern. Assoc. Great Lakes Res., 640-653.
- Smith, N. P., 1972: Summertime temperature and current characteristics of central Lake Superior. Ph.D. dissertation, University of Wisconsin, Madison.
- , and R. A. Ragotzkie, 1970: A comparison of computed and measured currents in Lake Superior. *Proc. Thirteenth Conf. Great Lakes Res.*, Intern. Assoc. Great Lakes Res., 969-977.
- Sonu, C. J., 1972: Field observations of nearshore circulation and meandering currents. *J. Geophys. Res.*, **77**, 3232-3247.
- Stommel, H., 1966: *The Gulf Stream*. Berkeley, University of California Press, 248 pp.
- Webster, F., 1961: The effect of meanders on the kinetic energy balance of the Gulf Stream. *Tellus*, **13**, 392-401.
- Whittaker, T. M., 1974: A simplified grid interpolation scheme for use in atmospheric budget studies. Ph.D. dissertation, University of Wisconsin, Madison (in preparation).
- Wolf, P. R., and T. J. Keating, 1973: Precise velocity measurements using photogrammetric techniques. *Water Res. Bull.*, **9**, 312-319.
- Yeske, L. A., 1973: The structure of the Keweenaw Current by photogrammetry. Ph.D. dissertation, University of Wisconsin, Madison.
- , T. Green, F. L. Scarpance and R. E. Terrell, 1972: Current measurements in Lake Superior using aerial photogrammetric techniques: A preliminary report. *Proc. Fifteenth Conf. Great Lakes Res.*, Intern. Assoc. Great Lakes Res., 689-697.
- , —, and —, 1973: On current measurements in Lake Superior by photogrammetry. *J. Phys. Oceanogr.*, **3**, 165-167.